

Soluble Surfactants Undergoing Surface Phase Transitions: A Maxwell Construction and the Dynamic Surface Tension

James K. Ferri and Kathleen J. Stebe¹

Department of Chemical Engineering, Johns Hopkins University, 3400 North Charles Street, Baltimore, Maryland 21218

Received August 14, 1997; accepted September 17, 1998

The dynamic surface tension of a soluble surfactant which undergoes a surface phase transition from a gaseous to a liquid expanded state is described. The application of a Maxwell construction to the surface equation of state is used to implicitly locate C^* , the bulk concentration at which the surface phase transition occurs, and the binodal surface concentrations Γ^G and Γ^L . The dynamic surface tension is assumed to reflect the instantaneous surface concentration. The mass transfer of surfactant to the interface is modeled as being controlled by bulk diffusion, or the kinetics of adsorption–desorption, or both, in a manner that accounts for the constant chemical potential as the interface undergoes the phase change and the differing interaction energies in the surface phases. As an example, using the Frumkin equation, equilibrium data for the surfactant 7-tetradecyn-6,9-diol are fitted for the maximum surface concentration Γ_∞ , the ratio of the characteristic kinetic constants for adsorption and desorption β/α , and intermolecular interaction parameter K . The Maxwell construction then dictates C^* , Γ^G , and Γ^L . These constants are then used to interpret dynamic surface tension data. The binodal concentrations are discussed in terms of the characteristic area swept out by the adsorbed molecule at the interface. Finally, the surface tension evolution is shown to be consistent with diffusion-controlled adsorption. © 1999 Academic Press

Key Words: dynamic surface tension; surfactants; kinetic constants for adsorption–desorption; intermolecular interactions; surface phase transitions; induction times; Maxwell construction.

1. INTRODUCTION

Transitions from gaseous to liquid expanded surface phases have long been understood to occur in insoluble monolayers spread at liquid–gas interfaces (1). For soluble surfactants, surface phase changes in adsorbed layers have also been predicted and discussed in terms of the equilibrium surface tension as a function of bulk concentration (2–4). The occurrence of these transitions for soluble surfactants has been confirmed by the direct visualization of coexisting surface phases using surface microscopy techniques (5–7).

Consider first an insoluble amphiphile spread to form a monolayer at a liquid–gas interface. Below a critical temperature, the amphiphiles can undergo a first-order surface phase

change from a gaseous to a liquid-expanded state. When the monolayer is compressed isothermally and slowly from the gaseous state, the surface pressure increases until the amphiphile attains a binodal gaseous surface concentration, Γ_G . Thereafter, as the compression proceeds, the surface pressure remains constant as the interface enters a region of two-phase coexistence. Islands of liquid-expanded phase at the binodal surface concentration Γ_L grow in the continuous gaseous phase. This proceeds until the interface is covered with the liquid-expanded phase at Γ_L . Further compression in the liquid-expanded phase causes the surface pressure to increase.

Consider now a soluble surfactant which undergoes a surface phase transition. When the surfactant adsorbs onto an initially clean interface, the surface tension has an induction period before it decreases to attain equilibrium. The relevance of this induction period was discussed by Lin *et al.* (8). The delivery of surfactant to the interface by diffusion and adsorption increases Γ . Initially, Γ is less than Γ_G , and adsorption weakly decreases the surface tension γ . When Γ reaches Γ_G , the interface enters a two-phase coexistence region; γ remains constant as surfactant adsorbs. Islands of liquid-expanded phase at Γ_L grow until the surface is covered. Further adsorption increases Γ and decreases the surface tension γ .

In both scenarios, the dependence of γ on Γ is determined by the surface equation of state. For the insoluble monolayer, a Maxwell construction can be performed on the surface equation of state to locate the surface binodal concentrations Γ_L and Γ_G (9). For the soluble surfactant, the same construction can be performed (2). Since the equation of state is related to the bulk concentration through the Gibbs' adsorption equation, C^* , the bulk concentration at which the surface phase change occurs, is also found.

In Lin's original study, and in further work undertaken on the dynamic surface tension of phase-changing surfactants (7, 8), a piecewise approach has been taken for the adsorption isotherm and surface equation of state. In this article, a Maxwell construction applied to a single surface equation of state is discussed in the context of equilibrium and dynamic surface tensions. This approach is valid for any isotherm capable of predicting the onset of a phase transformation and is demonstrated here using a Frumkin model.

Below, the thermodynamic arguments behind locating the

¹ To whom correspondence should be addressed.

binodal surface concentrations are briefly reviewed. The implications of these relationships in the behavior of γ vs $\ln C_\infty$ are discussed. Assuming local state and a mass transfer model for surfactant adsorption at the interface, the surface tension evolution for a soluble molecule which undergoes a surface phase change is predicted. The model assumes mixed kinetic-diffusion control. This model recovers the limits of diffusion-control when adsorption-desorption are sufficiently rapid, and pure kinetic control when they are sufficiently slow.

The diffusion-controlled model is compared favorably to equilibrium and dynamic data taken for the surfactant 7,8-tetradecyn-7,8 diol; diffusivities D agree well with that found by PFGSE NMR (10). Using the value of $D = 6.7 \times 10^{-6}$ cm²/s, a bounding value for the kinetic constant for desorption α is calculated. Desorption can be as slow as 0.1 s⁻¹ and still yield apparently diffusion-controlled surface tension relaxations.

2. EQUILIBRIUM: A MAXWELL CONSTRUCTION FOR AN INTERFACE

For a Gibbs' dividing surface of zero thickness, the surface excess Helmholtz free energy is defined as

$$F^s = \gamma A + \sum N_i^s \mu_i, \quad [1]$$

where N_i^s and μ_i are the surface excess moles and the chemical potential of component i , respectively; γ is the surface tension; and A is the area of the interface. When we locate the dividing surface such that the surface excess moles of the solvent are zero and consider a single surface active component, Eq. [1] can be recast:

$$\mu = f^s - \gamma a. \quad [2]$$

In this equation,

$$f^s = \frac{F^s}{N^s} \quad [3]$$

and

$$a = \frac{A}{N^s}; \quad \Gamma = \frac{1}{a}, \quad [4]$$

where Γ is the surface excess of the surfactant per unit area.

For a surface gaseous phase (G) in equilibrium with a surface liquid-expanded phase (L), the chemical potentials of the two surface phases must be equal:

$$f_L^s - f_G^s = \gamma(a_L - a_G). \quad [5]$$

Noting that

$$\left(\frac{\partial f}{\partial a} \right)_T = \gamma, \quad [6]$$

Eq. [5] can be written as

$$\int_{a_L}^{a_G} \gamma da = \gamma(a_G - a_L). \quad [7]$$

Equation [7] locates the binodal concentrations. Functions relating γ and a are of the form presented in Fig. 1a if surfactant interactions are sufficiently pronounced. That is, there is an (unstable) region of oscillatory behavior in γ . The tie line between binodal concentrations is located by the solution of Eq. [7]; the two endpoints give the binodal concentrations, $a_G = 1/\Gamma_G$ and $a_L = 1/\Gamma_L$. The surface tension remains constant at the tie line value for $\Gamma_G < \Gamma < \Gamma_L$, obeying the solid curve in Fig. 1a.

The coexisting surface phases are at equilibrium with the bulk surfactant solution, and thus occur at a single bulk concentration, C^* . Therefore, the adsorption isotherm governing $\Gamma(C)$ must be piecewise continuous at C^* . Typically, as shown in Fig. 1b, adsorption isotherms that capture surface phase changes have multiple solutions for Γ at C^* , only two of which (the binodal concentrations) are also solutions to the Maxwell construction.

The adsorption isotherm is related to the surface equation of state for γ by the Gibbs' adsorption equation:

$$\frac{\partial \gamma}{\partial \mu} = -\Gamma. \quad [8]$$

At C^* there is a discontinuity in the slope of γ vs $\ln C_\infty$:

$$\lim_{C_\infty \rightarrow C^{*-}} \frac{\partial \gamma}{\partial \mu} = -\Gamma_G, \quad [9a]$$

$$\lim_{C_\infty \rightarrow C^{*+}} \frac{\partial \gamma}{\partial \mu} = -\Gamma_L. \quad [9b]$$

However, the surface tension is continuous:

$$\gamma(\Gamma_G) = \gamma(\Gamma_L). \quad [10]$$

Models for the surface tension as a function of bulk concentration which predict phase transitions also have multiple solutions of $\gamma(C^*)$. However, only one satisfies both Eqs. [9] and [10]; this solution is labeled “*” in the inset of Fig. 2. The resulting solution for γ vs $\ln C_\infty$ is shown as the solid curve.

To illustrate these concepts, the Frumkin adsorption isotherm and the corresponding surface equation of state are

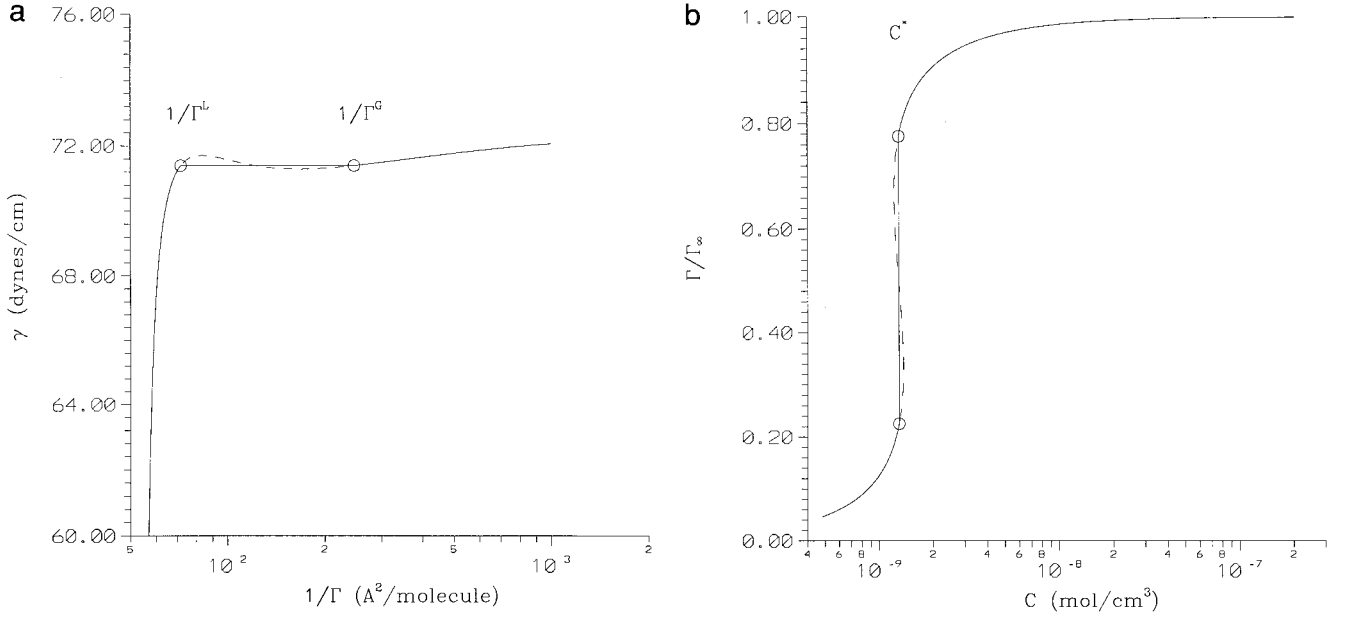


FIG. 1. (a) Surface tension γ vs specific area $1/\Gamma$ using the Frumkin equation of state. The dashed line represents the unmodified equation, and the solid line is the equation modified by the Maxwell construction with the gaseous ($1/\Gamma^G = 247 \text{ \AA}^2$) and the liquid ($1/\Gamma^L = 72 \text{ \AA}^2$) binodal specific areas shown. (b) The surface coverage Γ vs bulk concentration C for the Frumkin adsorption isotherm. The binodal coverages are indicated by the open circles along the vertical line located at the coexistence bulk concentration C^* .

adopted. These equations apply for monolayer adsorption in the limit of dilute C_∞ for which the bulk solution can be treated as ideal.

$$x = \frac{k}{e^{Kx} + k}, \quad [11]$$

where

$$k = \frac{\beta C_\infty}{\alpha}, \quad x = \frac{\Gamma_{\text{eq}}}{\Gamma_\infty}. \quad [13]$$

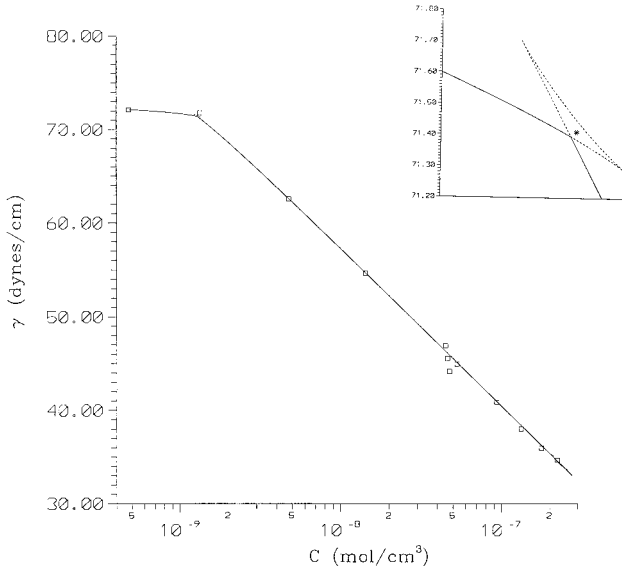


FIG. 2. Surface tension γ vs bulk concentration C as predicted by the Frumkin equation for values of $\beta/\alpha = 8.18 \times 10^7 \text{ cm}^3/\text{mol}$, $\Gamma_\infty = 2.98 \times 10^{-10} \text{ mol/cm}^2$, and $K = -4.5$. The symbols represent data taken using the pendant bubble apparatus for the acetylenic diol. The inset shows the implicit calculation of the Maxwell construction.

In these expressions, Γ_∞ is the maximum monolayer surface concentration (the inverse minimum area/molecule); Γ_{eq} is the equilibrium surface concentration. The parameters α and β are the characteristic kinetic constants for desorption and adsorption, respectively. The adsorption number k , a scaled concentration, is the ratio of characteristic adsorption to desorption rates. The parameter K accounts for nearest neighbor interactions among adsorbed surfactants. For cohesive interactions, $K < 0$. The fraction of interface covered by surfactant at equilibrium with a given k and K is denoted x . In Eq. [12], γ_0 is the surface tension of the pure solvent interface. (In order to describe the equilibrium surface tension at a given interface using the Frumkin model, values for γ_0 , Γ_∞ , K , and β/α must be known for the system.) Equation [12] is graphed in Fig. 1a; Eq. [11] is graphed in Fig. 1b. Using Eqs. [11]–[13], $\gamma(C)$ is graphed in Fig. 2.

Equation [12] can be recast in terms of the surface pressure $\pi = \gamma_0 - \gamma$:

$$\frac{\pi}{RT\Gamma_\infty} = -\left[\ln(1-x) - \frac{K}{2}x^2\right]. \quad [14]$$

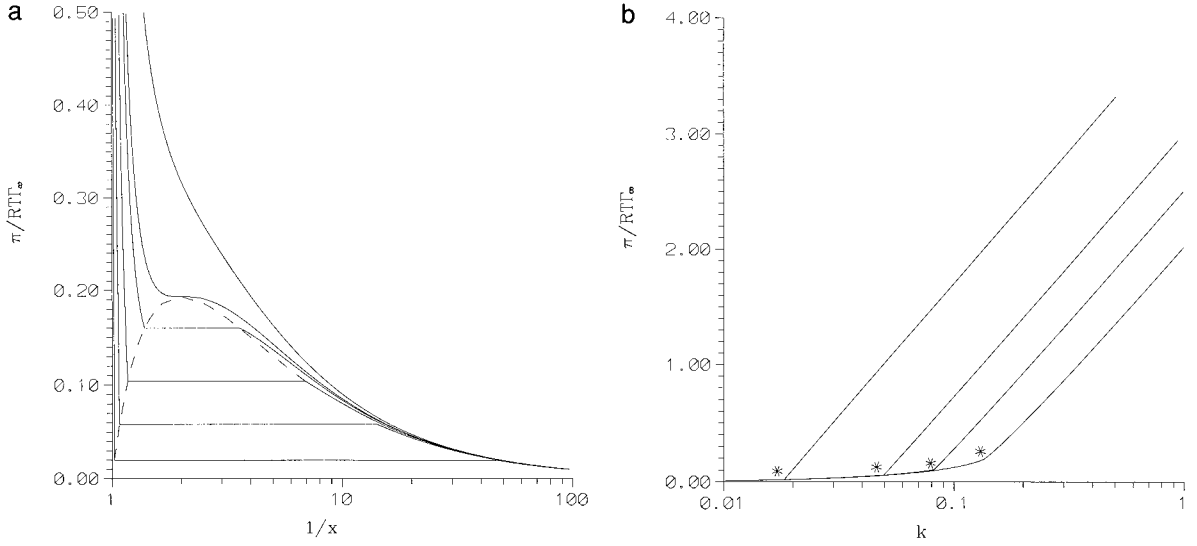


FIG. 3. The equilibrium behavior of the interface as a function of the strength of the interactions for $K = -3, 0, -4.0, -4.3, -5.0, -6, -8$; the * indicates the location of k^* for each K value. (a) $\pi/RT\Gamma_\infty$ vs $1/x$; (b) $\pi/RT\Gamma_\infty$ vs k .

Frumkin (2) showed that for $K = -4$, the system exhibits critical behavior, and for $K < -4$, Eq. [14] exhibits the oscillatory behavior shown in the inset to Fig. 1a. Using a Maxwell construction, $x_G = \Gamma_G/\Gamma_\infty$ and $x_L = \Gamma_L/\Gamma_\infty$ can be located; $k^* = \beta C^*/\alpha$ is then given by the solution of Eq. [11] at these coverages. The equation of state resulting from this calculation is shown in Fig. 2. Note that the binodal calculation must predict the same k^* as one would obtain from simply requiring that the surface tension in Fig. 2 be a continuous and single valued function of the bulk concentration. This is analogous to pressure and chemical potential for bulk phase changes in three dimensions (11).

The magnitude of intermolecular cohesion K can be varied, for example, by studying a homologous series of n -alcohols as a function of chain length. In order to investigate the impact of increasing cohesion on the equilibrium behavior of this system, Eq. [14] is graphed as a function of K in Fig. 3a, where the Maxwell construction was used to locate the tie line for each K value. The tie lines become longer as cohesion is increased; i.e., x_G decreases and x_L increases. The location of the coexistence surface pressure $\pi^* = \gamma_o - \gamma^*$ also shifts; the surface tension reduces less before entering the coexistence region. The strength of cohesive interactions also alters the surface tension as a function of the bulk concentration, k . In Fig. 3b a family of normalized surface pressure vs k curves are graphed as a function of K . The k^* are indicated by the “*” symbol; the coexistence bulk concentrations decrease as cohesion increases.

3. MASS TRANSFER AND THE DYNAMIC SURFACE TENSION

Adsorption to a Single Phase Interface

Adsorption to an initially clean interface of a pendant bubble formed in a surfactant solution of bulk concentration C_∞ is

modeled. The surface concentration $\Gamma(t)$ is initially zero; at long times it attains its equilibrium value Γ_{eq} . Surfactant in the sublayer adjacent to the interface adsorbs, thereby depleting the sublayer concentration C_s and causing surfactant to diffuse from the bulk toward the interface. For diffusion from the bulk, the evolution of $\Gamma(t)$ is (12)

$$\Gamma(t) = 2\sqrt{\frac{D}{\pi}} \left[C_\infty \sqrt{t} - \int_0^{\sqrt{t}} C_s(t - \tau) d\sqrt{\tau} \right] + \frac{D}{A} \left[C_\infty t - \int_0^t C_s(\tau) d\tau \right], \quad [15]$$

where A and D are the bubble radius and surfactant bulk diffusivity, respectively. Surfactant in the sublayer must overcome a kinetic barrier to adsorption. For a single phase interface, the kinetic barrier for a surfactant obeying a Frumkin isotherm can be expressed:

$$\frac{\partial \Gamma}{\partial t} = \beta C_s (\Gamma_\infty - \Gamma) - \alpha e^{(K(\Gamma)/\Gamma_\infty)} \Gamma, \quad [16]$$

which assumes that cohesion (i.e., K) increases the activation energy for desorption.

These equations are recast in dimensionless form according to

$$C' = \frac{C}{C_\infty}; \quad \Gamma' = \frac{\Gamma}{\Gamma_{eq}}; \quad r' = \frac{r}{A}; \quad t' = \frac{t}{\tau_D}; \quad \gamma' = \frac{\gamma}{RT\Gamma_\infty}. \quad [17]$$

The diffusion time scale τ_D is defined as

$$\tau_D = \frac{h^2}{D}, \quad [18]$$

where

$$h = \frac{\Gamma_{\text{eq}}}{C_{\infty}}. \quad [19]$$

The dimensionless equations governing the $\Gamma'(t')$ and $\gamma'(t')$ are

$$\begin{aligned} \Gamma'(t') = & \frac{2}{\sqrt{\pi}} \left[\sqrt{t'} - \int_0^{\sqrt{t'}} C'_s(t' - \tau') d\sqrt{\tau'} \right] \\ & + \frac{h}{A} \left[t' - \int_0^{t'} C'_s(\tau') d\tau' \right], \end{aligned} \quad [20]$$

$$\frac{d(x\Gamma')}{dt} = \Lambda [kC'_s(1 - x\Gamma') - e^{(Kx\Gamma')}x\Gamma'], \quad [21]$$

$$\gamma'(t') = \gamma'_0 + \ln(1 - x\Gamma'(t')) - \frac{K}{2} x^2 \Gamma'(t')^2. \quad [22]$$

In these expressions, nonideal interactions are assumed to alter desorption alone. The quantity $1/\alpha$ is the desorption kinetic time scale. The ratio of the diffusion time scale to the desorption time scale defines Λ :

$$\Lambda = \alpha\tau_D. \quad [23]$$

If $\Lambda \approx 1$, then both adsorption–desorption kinetics and diffusion control the mass transfer. If $\Lambda \ll 1$, kinetics alone control the mass transfer according to Eq. [21], with $C'_s = 1.0$ throughout the adsorption process. If $\Lambda \gg 1$, then diffusion alone controls the mass transfer according to Eq. [20]. In this limit, Eq. [21] reduces to

$$x\Gamma'(t') = \frac{kC'_s(t')}{e^{(Kx\Gamma')} + kC'_s(t')}, \quad [24]$$

i.e., the interface maintains equilibrium with the sublayer concentration C'_s . Below, this analysis is amended for an interface undergoing a phase transition.

Diffusion Controlled Flux to an Interface with a Phase Transition

When an interface is freshly formed in solution, surfactant diffuses to the sublayer and adsorbs according to the isotherm in Fig. 1b. Both C'_s and Γ' are initially zero. For $\Gamma' < \Gamma'_G$, Eqs.

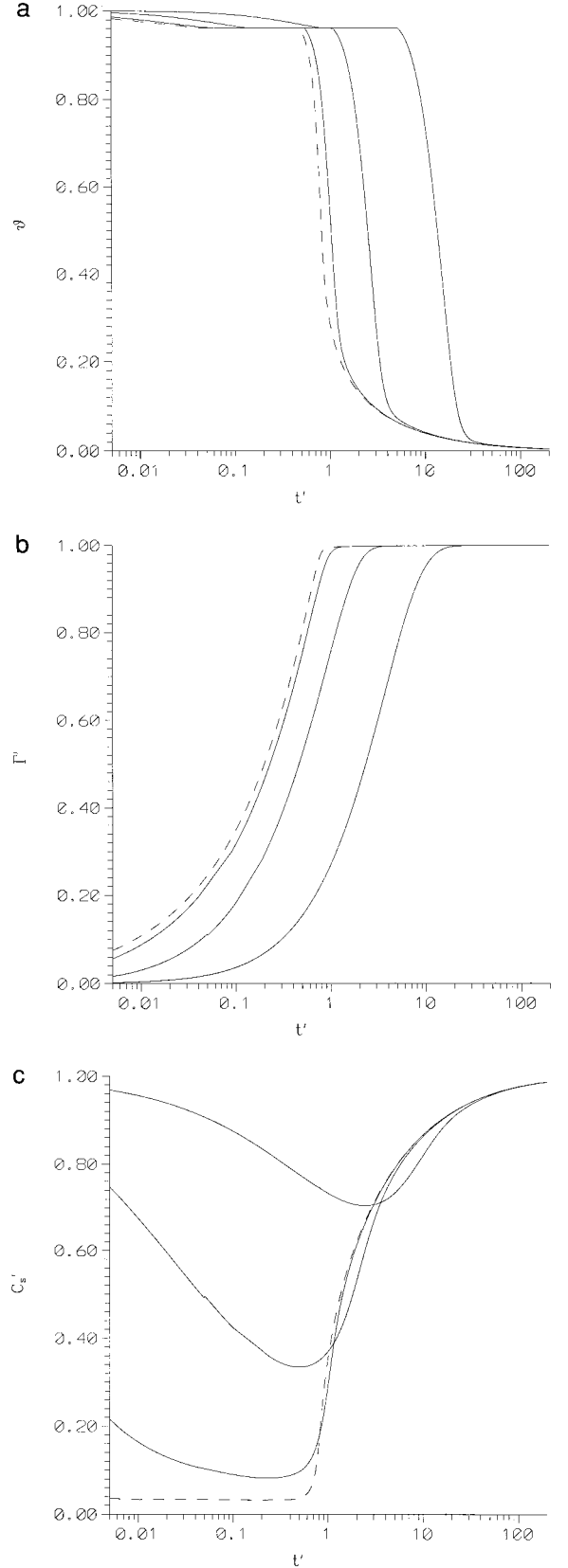


FIG. 4. The dynamic behavior of the interface as a function of Λ ($\Lambda = 0.8, 8, 80$) for fixed $k = 4.1$. The dotted line indicates the diffusion-controlled limit. (a) θ vs t' ; (b) Γ' vs t' ; (c) C'_s vs t' .

[20] and [24] determine Γ' ; Eq. [22] determines γ' . Both C'_s and Γ' increase monotonically from zero until the instant t^* when $\Gamma' = \Gamma'_G$ and $C'_s = C'^*_s$. At that time, Γ' increases along the vertical in the adsorption isotherm; γ' stays fixed at the coexistence surface tension. Domains of liquid-expanded phase grow until the entire interface is covered. Defining the fraction of the interface covered with surface gaseous phase as Φ , the surface concentration evolves according to a lever rule:

$$x\Gamma' = x_G\Phi + x_L(1 - \Phi); \quad \Phi(t^*) = 1.0, \quad [25]$$

where

$$x_G = \frac{\Gamma_G}{\Gamma_\infty}; \quad x_L = \frac{\Gamma_L}{\Gamma_\infty}. \quad [26]$$

During the phase transition, Γ' is determined from the simultaneous solution of Eq. [20] and the requirement that C'_s remain fixed at C'^*_s until $\Gamma' = \Gamma'_L$, and $\Phi = 0.0$. For $\Gamma' > \Gamma'_L$, C'_s and Γ' increase according to Eqs. [20] and [24]; γ' evolves according to Eq. [22] until equilibrium is attained.

Mixed Controlled Adsorption with a Surface Phase Change

If the rates of adsorption-desorption are slow, the sublayer can be strongly out of equilibrium with the interface. Initially, Γ' is zero and C'_s is unity. Surfactant adsorbs from the sublayer according to Eq. [21]. Diffusion determines C'_s ; Eqs. [20] and [21] are solved simultaneously until $\Gamma' = \Gamma'_G$ at $t = t^*$. At that time, Γ' increases according to the simultaneous solution of Eq. [20] and

$$\frac{d\Phi}{dt} = \frac{\Lambda}{x_G - x_L} \{kC'_s(1 - [x_G\Phi + x_L(1 - \Phi)]) - [e^{Kx_G}\Phi + e^{Kx_L}(1 - \Phi)]\}, \quad [27]$$

where Eq. [25] applies. This equation reflects that the energy barrier to desorption is different in the surface liquid and gaseous phases.

For $\Gamma' > \Gamma'_L$, C'_s and Γ' again evolve according to Eqs. [20] and [21]; γ' decreases according to Eq. [22] until equilibrium is attained.

Numerical Results

First consider the role of Λ in the dynamic surface tension for fixed k and K . The evolution of the surface tension γ' is reported in terms of the scaled variable θ , defined as

$$\theta = \frac{\gamma_0 - \gamma(t')}{\gamma_0 - \gamma_{eq}}. \quad [28]$$

The evolution of θ , Γ' , and C'_s are shown as a function of t' in Fig. 4a, b, and c, respectively. As Λ increases, the diffusion-

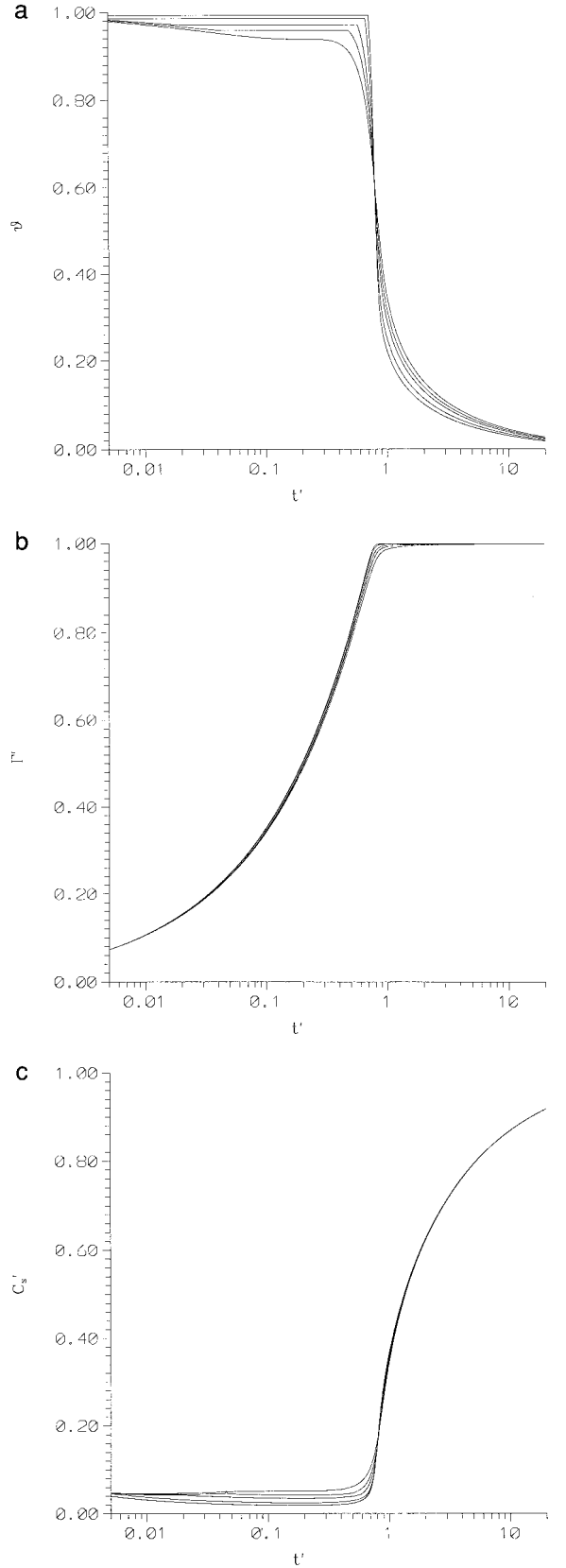


FIG. 5. The dynamic behavior of the interface as a function of K for $K = -4.0, -4.5, -6.0, -7.0$ for $k = 1.0$. (a) θ vs t' ; (b) Γ' vs t' ; (c) C'_s vs t' .

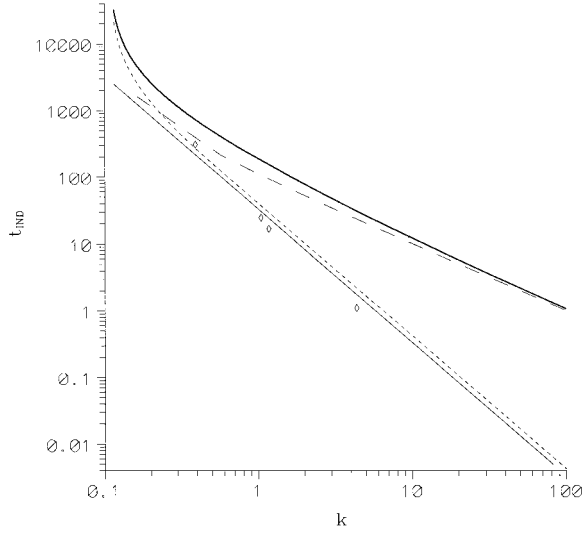


FIG. 6. The induction time t_{ind} vs $\ln k$ for the full diffusion-controlled solution (short dashed line), the approximate diffusion-controlled solution (solid line), kinetic control (long dashed line), and mixed diffusion-kinetic control (bold solid line). In this simulation, $\alpha = 0.015 \text{ s}^{-1}$, $D = 6.7 \times 10^{-6} \text{ cm}^2/\text{s}$, $\beta/\alpha = 8.18 \times 10^7 \text{ cm}^3/\text{mol}$, $\Gamma_\infty = 2.98 \times 10^{-10} \text{ mol}/\text{cm}^2$, and $K = -4.5$. The symbols represent the experimental values for t_{ind} as a function of k for the acetylenic diol.

controlled profile is recovered. The smaller is Λ , the slower is the adsorption process, and the longer is the induction period.

In order to understand the impact of increasing K on the dynamic behavior of the system, families of $\theta(t')$, $\Gamma'(t')$, and $C'_s(t')$ as a function of K at fixed concentration k for a diffusion controlled process are presented in Fig. 5a–c, respectively. The length of the induction time increases for larger K because of the increased tie line length.

Let the induction time t_{ind} be defined as the instant when $\Phi = 0$, i.e., when the interface is completely covered with the liquid expanded phase. The variation of t_{ind} in seconds with bulk concentration k is shown in Fig. 6 for fixed surfactant material parameters as given in the figure caption. These results are for the full simulations. For diffusion control, t_{ind} goes as k^{-2} at dilute concentrations. Note, however, that the result from the full solution differs from the result calculated from the short time approximation:

$$t_{\text{ind}} = \frac{\pi}{4D} \left(\frac{\Gamma_L}{C_\infty} \right)^2, \quad [29]$$

because of back-diffusion; these differences are particularly pronounced at dilute concentrations. For pure kinetic control, t_{ind} goes as k^{-1} . For mixed-control, t_{ind} varies from diffusion-controlled behavior for small k to kinetic controlled behavior at large k . Such a trend in t_{ind} has been observed in an experimental study of the surface phase behavior of the globular protein lysozyme (13). This occurs because at dilute concentrations, τ_D is long, and typically, $\Lambda \gg 1$. As concentration increases, τ_D decreases. If concentration is made high enough, Λ can be reduced sufficiently to drive the system into a kinetically controlled regime.

4. EXPERIMENTS

Materials

The 7,8-tetradecyn-7,8 diol was synthesized at Air Products and used without modification. A Millipore MilliQ water purification system was used to rinse all components and to make all solutions. This system provides water with a specific resistivity of greater than $18 \text{ M}\Omega \text{ cm}$. All glassware and Teflon components used in the experiments were soaked overnight in Nochromix cleaning solution. They were then thoroughly rinsed and dried in a protective cabinet. The needles were sonicated 4 times for 2 min in purified water using a rinse–sonicate–rinse protocol. Surfactant solutions were used within 7 days of preparation.

Protocol

The surface tension evolution is studied by the pendant bubble method (12). The apparatus consists of a quartz cell filled with surfactant solution. This cell is placed in the path of a collimated light beam. A bubble is formed on an inverted needle. The light beam casts a bubble silhouette onto a CCD camera; the bubble shadow is digitized and recorded to disk. The bubble shape is matched numerically to the Young–Laplace equation allowing γ to be determined. For dynamic studies, a bubble is rapidly formed (in less than 0.1 s) and the camera is set to strobe, obtaining the

TABLE 1

I. Equilibrium Parameters from Maxwell Construction			
$\beta/\alpha = 8.18 \times 10^7 \text{ cm}^3/\text{mol}$	$\Gamma_\infty = 2.98 \times 10^{-10} \text{ mol}/\text{cm}^2$	$K = -4.5$	
$x_G = 0.2246$	$x_L = 0.7758$	$C^* = 1.29 \times 10^{-9} \text{ mol}/\text{cm}^3$	
II. Best-Fit Kinetic Parameters			
$C_\infty \text{ (mol}/\text{cm}^3)$	$D \text{ (cm}^2/\text{s)}$	$\alpha \text{ (1/s)}$	$\alpha e^{Kx} \text{ (1/s)}$
4.78×10^{-9}	3.9×10^{-6}	3.9×10^{-2}	5.0×10^{-4}
1.43×10^{-8}	6.7×10^{-6}	2.95	3.9×10^{-2}
5.31×10^{-8}	6.5×10^{-6}	8.72	9.8×10^{-2}

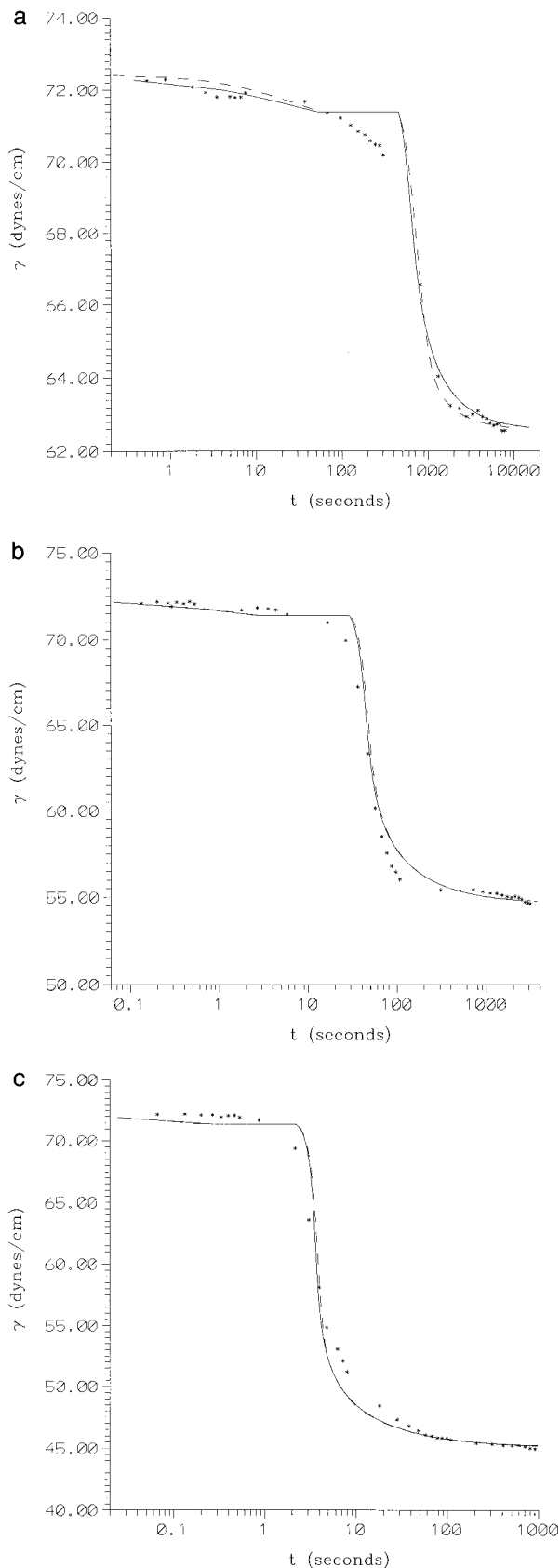


FIG. 7. Surface tension relaxation obtained by pendant bubble for 7,8-tetradecyn-6,9-diol at (a) $C_{\infty} = 4.78 \times 10^{-9}$ mol/cm³, (b) $C_{\infty} = 1.43 \times$

bubble shape as a function of time. The surface tension corresponding to each image is found. The long time asymptote is the equilibrium surface tension of the surfactant solution.

Results

The acetylenic diol surfactant has the characteristic behavior of a surfactant which undergoes a gaseous–liquid–expanded phase transition. This is suggested by the near cusp in the γ – $\ln C_{\infty}$ plot in Fig. 2 and the induction period in the dynamic traces in Fig. 7. The best fit equation of state is reported in the caption to Fig. 2. (Note that a slightly subcritical value for K would be able to describe the equilibrium tensions, but would not agree as well with the dynamic traces.) The specific area (247 Å²/molecule) corresponding to the onset of the phase transition can be compared with the area of a disk with the diameter (22 Å) of a fully extended diol (376 Å²). The diameter was calculated using literature values of the bond lengths between the stiff members of the carbon backbone. The length of extension of the saturated chain was calculated using average chain extension arguments in three dimensions (14).

The dynamic data are matched to a diffusion controlled mass transfer model, shown as the continuous curves in Fig. 7. The best fit values for D are reported in Table 1 for each concentration studied. They are in reasonable agreement with the surfactant self-diffusion coefficient as measured by PFGSE NMR, $D = 4.4 \times 10^{-6}$ cm²/s. This agreement implies that adsorption–desorption is sufficiently rapid that diffusion regulates the system behavior. In order to determine how rapidly molecules must desorb in order for this limit to hold, the data are also compared to a mixed-control model for fixed $D = 6.7 \times 10^{-6}$ cm²/s. The smallest values for α which agree with the data for each concentration are reported in Table 1. The greatest of these bounding values is $\alpha = 8.72$ s^{−1}; any value of $\alpha \geq 8.72$ s^{−1} will agree with all of the kinetic data reported. The prevailing kinetics of desorption are weighted by the Arrhenius activation energy term, estimated to be e^{Kx} . Thus, the prevailing desorption rate αe^{Kx} can be as slow as roughly 0.1 s^{−1} and still yield apparently diffusion-controlled relaxations. Finally, the values for t_{ind} measured in these experiments are plotted as symbols in Fig. 6 and found to agree well with the diffusion-controlled limit.

5. CONCLUSIONS

In this article, a Maxwell construction for a soluble surfactant is used to describe the dynamic surface tension as the surfactant adsorbs to an initially surfactant-free interface. A model assuming mixed kinetic-diffusion control for adsorption is generalized to include surface phase changes. The model recovers the diffusion-controlled limit in the limit of fast ad-

10^{-8} mol/cm³, and (c) $C_{\infty} = 5.31 \times 10^{-8}$ mol/cm³. The solid curve is the diffusion-controlled model prediction. The dashed curve is the mixed-control model for D fixed at 6.7×10^{-6} cm²/s. The best fit D and α are reported in Table 1.

sorption–desorption, and pure kinetic control in the limit of slow adsorption/desorption.

The induction time in the dynamic surface tension that is the signature of a surface phase change is shown to vary inversely with the square of the bulk concentration for diffusion-controlled adsorption, with the inverse bulk concentration for kinetic-control, and to go from agreement with diffusion-control at dilute concentrations to kinetic controlled behavior at elevated concentrations for mixed diffusion-kinetic control.

The model is compared favorably to the dynamic surface tension of a the surfactant 7-tetradecyn-6,9-diol, which is shown to obey diffusion control at the concentration studied. By comparing the dynamic trace to the mixed kinetic-diffusion control model, the desorption coefficient α is bounded.

ACKNOWLEDGMENTS

We thank Drs. Robert Stevens and Jeffrey DePinto, our collaborators at Air Products, Inc., for providing both technical and financial support, and Thomas Hocker for the many useful discussions concerning stability analyses.

REFERENCES

1. Gaines, G. L., "Insoluble Monolayers at Liquid–Gas Interfaces." Wiley-Interscience, New York, 1966.
2. Frumkin, A., *Z. Phys. Chem.* **116**, 446 (1925).
3. Aratono, M., Uryu, S., Hayami, Y., Motomura, K., and Matuura, R., *J. Colloid Interface Sci.* **98**, 33 (1984).
4. Israelachvili, J., *Langmuir* **10**, 3774 (1994).
5. Pollard, M. L., *et al.*, *Langmuir*. [In press].
6. Henon, S., and Meunier, J., *J. Chem. Phys.* **98**, 9148 (1993).
7. Melzer, V., and Vollhardt, P., *Phys. Rev. Lett.* **76**, 3770 (1996).
8. Lin, S., McKeigue, K., and Maldarelli, C., *Langmuir* **7**, 1055 (1991).
9. See Ter, Minsassian, Saraga, and Prigogine, in "Surface Tension and Adsorption" (R. Defay and I. Prigogine, Eds.). John Wiley & Sons, New York, 1966.
10. Stilbs, P., *Prog. NMR Spectrosc.* **19**, 1 (1985).
11. See, for example: Callen, H., "Thermodynamics," p. 150. John Wiley & Sons, New York, 1960.
12. Lin, S., McKeigue, K., and Maldarelli, C., *AIChE J.* **36**, 1785 (1990).
13. Sundaram, S., *et al.*, *Langmuir* **14**, 1208–1218 (1998).
14. Hiemenz, P., "Principles of Colloid and Surface Chemistry," 2nd ed., Marcel Dekker, Inc., New York, 1986.